SYNTHESIS, CHARACTERIZATION AND DYE REMOVAL PROPERTIES OF CELLULOSE NANOCRYSTALS EMBEDDED NATURAL RUBBER LATEX COMPOSITE

AISWARYA R. NAIR, SREEDHA SAMBHUDEVAN and BALAKRISHNAN SHANKAR*

Department of Chemistry, Amrita Vishwa Vidyapeetham, Amritapuri, India
*Department of Mechanical Engineering, Amrita Vishwa Vidyapeetham, Amritapuri, *India*
✉ *Corresponding author: Sreedha Sambhudevan, sreedha@am.amrita.edu*

Received February 5, 2018

Cellulose nanocrystals (CNCs) were prepared from bleached wood pulp by the acid hydrolysis method. CNCs were characterized by Fourier Transform Infrared Spectroscopy (FTIR) and X-Ray Diffraction (XRD). Natural rubber latex was oxidised using potassium permanganate. The oxidation of latex was confirmed using FTIR and UV-Visible Spectroscopy. Natural rubber latex composites were prepared using the as-prepared CNCs in two different weight percentages. Mechanical studies and microscopy analysis proved that the incorporation of CNCs into NR latex improved all the properties. Due to the presence of surface hydroxyl groups of CNCs, which can be exchanged with almost any contaminant ions present in water, the developed materials can be utilized for water purification. The composites effectively removed 92%, 79% and 67%, respectively, of basic dyes such as Victoria blue BO, Methyl violet 10B and Holacryl pink FG. The dye removal can be explained by the electrostatic attraction between the negatively charged CNCs and the positively charged dyes.

Keywords: cellulose nanocrystals, natural rubber latex, nanocomposites, dye removal

INTRODUCTION

Even though water is a renewable source, its quantity has not changed globally for the past 2000 years. Moreover, only three percent of the available water is fresh and one third of it is inaccessible. To make matters worse, the water available is often contaminated with effluents from industries, agriculture and households, especially, from dyes and pigment industries.[1] Dyes are very important chemicals and because of their complex structure, they are non-biodegradable, and hence their removal from water is not an easy task.[2]

Purifying water using today's technology is performed by techniques such as osmosis/reverse osmosis, various filtration processes, UV sterilization, ozonolysis, distillation *etc*. Most of them involve the use of non-biologic origin, non-recyclable and harmful to the environment materials, as well as have high energy requirements. Thus, it is undoubtful that there is a high need to research into innovative measures to clean water at lesser costs, using reduced energy, while reducing the harsh impacts on the environment.[3]

Polymer nanocomposites are a new range of materials that are promising for water purify-cation. Nanotechnology is the field where almost all branches of science are incorporated, exploiting the characteristic properties of materials in the nanoscale range. A major field of application of nanoparticles are in the manufacture of composites, which have proven to be manyfold superior to the conventional macro-/micro-polymer composites.[4] The selection of a suitable filler and matrix phase plays a vital role in the effectiveness of the end use of the developed composites.[5] Composites containing biological polymers, instead of synthetic polymers, are more eco-friendly. However, many of the already developed biopolymers lack a variety of desirable properties exhibited by synthetic polymers. Therefore, their reinfor-cement and the improvement of their properties are much needed and always an area of interest for scientists. Recent studies have proven that certain commonly used nanoparticles (NPs), such as carbon nanotubes (CNTs), TiO_2, *etc*., can be

toxic and need to be substituted with non-toxic ones. Bionanoparticles (BNPs) can be used to tackle this problem. BNPs are simply nanoparticles of biological origin and are potentially less toxic than their precursors. By the combination of a biopolymer as matrix and BNPs as fillers, one can develop a desired bionanocomposite (BNC).[7] BNCs are a new type of nano-sized materials, which provide a great array of benefits, such as non-toxicity, biocompatibility, availability of raw materials, ease of synthesis, flexibility and almost zero-pollution.

Cellulose nanocrystals (CNCs) are needle-type cellulose units with one dimension in the nano-range, with highly crystalline nature. These nanomaterials of biological origin present interest due to their exclusive structural properties and striking physicochemical peculiarities, such as biocompatibility, biodegradability, renewability, low density, adaptable surface chemistry, optical transparency and improved mechanical properties.[8] They are perfect candidates for a wide variety of applications, such as biomedical, pharmaceuticals, electronics, barrier films, nanocomposites, membranes, super-capacitors, *etc*.[9-11] In addition, the excellent properties of CNCs make them an excellent candidate for water purification.[12-14] The hydrophilic nature of cellulosic nanostructures are highly appreciated in reducing bio- and organic fouling.[15-16] Literature review have shown that incorporating organic functional groups into nanocellulose is highly useful in selective uptake of contaminants and hence water purification.[17-19] Researchers are also developing some novel methods of utilising cellulose in different ways. The synthesis of porous carbon from cellulose for dye absorption, cellulose/chitosan composite films for anionic dye removal and utilization of TEMPO-oxidised cellulosic fractions for dye removal are some of the recent trends in this area.[20-22]

In the present work, CNCs were prepared from wood pulp and natural rubber latex was used as matrix material to synthesize CNC/natural rubber nanocomposites, which can be used as a promising material for water purification.

EXPERIMENTAL

Materials and methods

Bleached wood pulp was received from Hindustan Newsprint Ltd., Velloor, Kerala. Laboratory grade formic acid and HCl, as well as natural rubber (NR) latex, with dry rubber content of 60%, was purchased from Sacharia Latex Exporters, Kottayam, Kerala. $KMnO_4$ crystals of laboratory grade were also used.

CNC preparation

Two grams of bleached chemical pulp was added to a mixture of 90% HCOOH and 10% HCl, and then vigorously agitated to obtain a pulp-like slurry. Later, the reaction was carried out in a round bottom flask (250 mL) kept in an oil bath at 95 °C for 30 min, with magnetic stirring at 900 rpm. On finishing the reaction, the flask was instantly cooled to room temperature, using water, and centrifuged until the mixture yielded a clear supernatant liquid. The solid residue was collected and dissolved in 100 mL distilled water, which was freeze-dried on a Freezone 2.5 Labconco Freeze Dry System.

NRL oxidation

A $KMnO_4$ solution was used to oxidise the NR latex. An aqueous solution of 0.125 mol L^{-1} $KMnO_4$ was prepared and diluted to 0.0125 and 0.00125 mol L^{-1}, and then added dropwise to the NR latex suspension under stirring, so as to achieve the oxidation of the double bonds present in the isoprene monomer. The typical colour variation of the solution from pink to brown and the formation of solid MnO_2 indicated that the oxidation process was over.

Preparation of composite film

An aqueous suspension of CNCs was made neutral and the NR latex was added in different quantities at normal temperature, and was uniformly mixed to get a good dispersion. The mixture was kept in vacuum and agitated on a Rotavapor for 10 min, to degas the mixture and to avoid the development of permanent foams in the course of water evaporation. Thin films of identical thickness were attained by casting on a glass mould and was evaporated at 40 °C in an oven for 4-6 hours and then heated at 60 °C for 2 days. The resultant films were stored at room temperature in a desiccator with $CaCl_2$. The films containing 2% CNC and 4% CNC were prepared similarly and then characterised with regard to their properties.

Fourier Transform Infrared Spectroscopy (FTIR)

FTIR was performed using a Perkin Elmer Spectrum Two-FTIR spectrophotometer in the range of 4000-400 cm^{-1}. The particles were powdered well and embedded in KBr crystals before taking the spectra. A pressure of 65-105 MPa was applied to get a transparent disc. The FTIR spectra of latex and oxidized latex were also taken using the Attenuated Total Reflection (ATR) method.

X-Ray Diffraction (XRD)

The XRD patterns of the samples were taken at room temperature on a Bruker AXS D8 Advance diffractometer, using a Ni filter, and equipped with a Cu X-ray source, at a wavelength of 1.5406 Å,

generator voltage of 60 kV and generator current of 40 mA. The samples were scanned at a step size of 0.020 2θ and step time 32.8 seconds.

Scanning Electron Microscopy (SEM)

Surface morphology was studied by means of a FEI Quanta 200 scanning electron microscope, using 5 keV secondary electrons. With liquid nitrogen, the samples were cryogenically fractured, followed by gold plating to minimize surface charging.

UV-Visible Spectroscopy

UV-visible absorption spectroscopy was employed to study the optical properties of the prepared samples, using a Perkin Elmer LAMBDA 265 UV-Vis spectrophotometer in the range of 300-700 nm.

Mechanical properties

Tensile strength was measured according to ASTM method D412-98 and tear strength – according to ASTM method D624-98, on an Instron 4411 (England) Universal Testing Machine (UTM) at a cross head speed of 500 mm/min and 100 mm/min, respectively. Tensile tests were done using dump-bell shaped samples and tear tests were done using crescent shaped specimens.

RESULTS AND DISCUSSION

FTIR analysis

Figure 1 shows the FTIR spectrum of CNCs, while Figure 2 presents an enlarged view of the spectrum. The spectrum exhibits a band at 3342 cm^{-1} that corresponds to the free O–H stretching vibration of the OH groups in cellulose. The spectrum indicates the characteristic C–H stretching vibration around 2905 cm^{-1}. The vibration peak detected at 1507 cm^{-1} is due to the CH_2 scissoring motion in cellulose, that at 1462 cm^{-1} is due to C-H bending, that at 1430 cm^{-1} is due to in-plane O-H bending, the peak at 1322 cm^{-1} is due to CH_2 wagging, and that at 1035 cm^{-1} is related to C–O–C stretching vibration in the pyranose ring. A close analysis reveals a peak in the region between 902-893 cm^{-1}, which is associated with the cellulosic β-glycosidic linkages.[23] The peak at 1160 cm^{-1} is due to C–C ring stretching, and that at 1110 cm^{-1} is due to the C–O–C glycosidic ether band. The absorbance peaks observed in the spectra of cellulose fibres, in the region of 1645 cm^{-1}, were attributed to the O–H bending of the adsorbed water. The somewhat higher moisture content is due to the absorption of water in the void spaces formed by the removal of hemicellulose and lignin. Lastly, the peak found in the spectra between 1040 and 1109 cm^{-1} is attributed to the C–O–C pyranose ring stretching vibration.[24]

Figures 3 and 4 illustrate the FTIR spectra of NR latex and oxidised NR latex, respectively. The absorption at 831 cm^{-1} indicates out-of-plane =CH bending of cis-1,4-. The corresponding peak in oxidized NRL proves the effective oxidation of the double bonds. A closer examination of the infrared spectra discloses the absorbance band at 1219 cm^{-1}, corresponding to O-P-O asymmetric stretching of phospholipids, signifying the presence of related phospholipids at the rubber chain. The absorption bands at 1367 cm^{-1} and 1447 cm^{-1} (C-H bending) are features of CH_2 distortion. The absorption band at 1645 cm^{-1} resembles C=C stretching in cis-1,4-polyisoprene. This peak is also found in the spectrum of oxidised NRL, at 1644 cm^{-1}, with a lower intensity, due to the oxidation of surface molecules only. This property is highly appreciated since the final composite will have the required characteristics of NR, keeping in mind that the extent of oxidation can be varied as per the requirements. The CH_2 symmetric stretching vibrations are observed in the region of 2855 cm^{-1}. The CH_3 asymmetric stretching in the spectrum of NRL is observed at 2955 cm^{-1}. In addition, the spectrum also shows a broad peak at around 3200-3500 cm^{-1}. This absorption band might be related to the presence of a hydroxyl group, since latex is an emulsion of polymer microparticles in an aqueous medium. The peak at 1744 cm^{-1} present in the NR sample is related to the molecules available on the outer part of latex particles. There is a slow decrease in the intensity of this peak as the oxidation level rises, confirming that these surface molecules are oxidized during the reaction.

XRD analysis

X-ray diffraction patterns of CNCs are shown in Figure 5. Particle size was calculated using Scherer's equation, $D = k\,\lambda / B\cos\theta$, where D is the particle size, K is a constant called dimensionless shape factor, λ is the wavelength of the X-ray used, B is line broadening at half the maximum intensity and θ is the Bragg angle. The calculated values for the particle size are listed in Table 1.

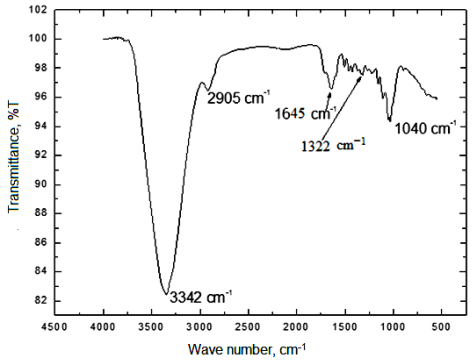

Figure 1: FTIR spectrum of CNCs

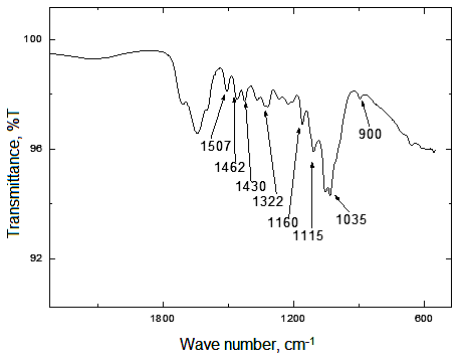

Figure 2: Enlarged FTIR spectrum of CNCs

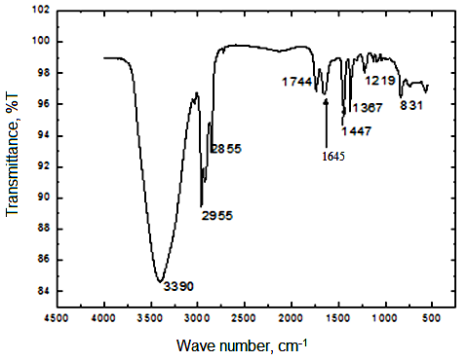

Figure 3: FTIR spectrum of NR latex

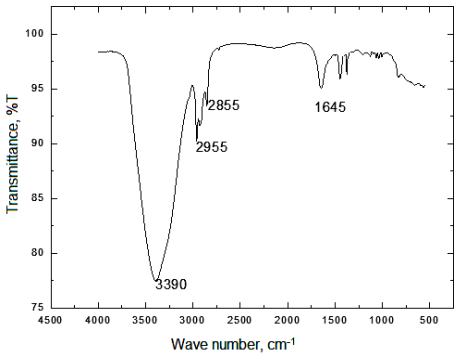

Figure 4: FTIR spectrum of oxidised NR latex

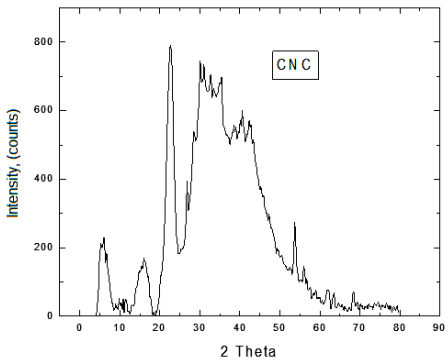

Figure 5: XRD pattern of CNCs

Table 1
Calculated particle size values of CNCs

2θ	FWHM	λ	D
53.714	0.391	0.15406	23.1
26.8	0.282	0.15406	29.5
22.59	1.805	0.15406	24.5

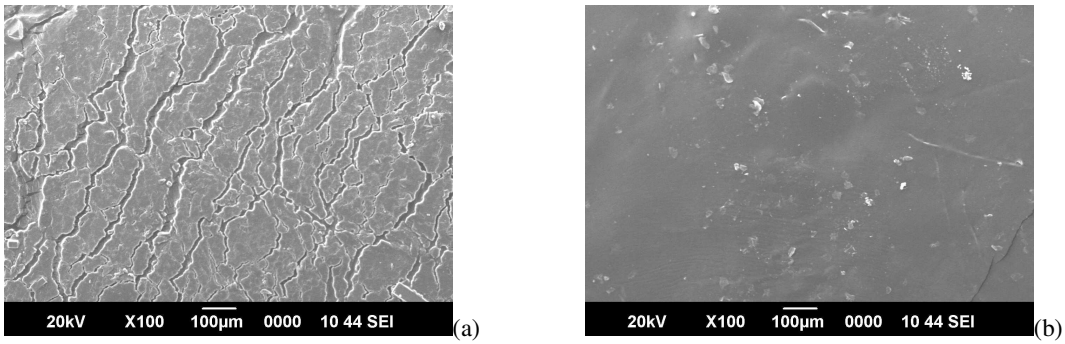

(a) (b)

Figure 6: SEM micrographs of (a) latex film and (b) composite film

Average particle size was calculated using Scherer's equation and was found to be 25.7 nm. The nanometre-sized crystalline particles proved that the hydrolysis was effective and the amorphous region of cellulose was removed successfully.

SEM

From the SEM micrographs presented in Figure 6, it is clear that the introduction of CNCs into rubber latex increases the homogeneity of latex particles in the composite. A homogeneous distribution of CNC particles in the latex can be observed from the SEM images, which is essential for the optimum properties of latex composites. The increase in homogeneity is also supported by the studies of the mechanical properties of the nanocomposites.

UV-Vis analysis

New –OH groups are introduced in the NR matrix through permanganate oxidation. It is assumed that 1 mole of $KMnO_4$ can produce 2 moles of new –OH groups *via* the oxidation reaction of the polymer, the concentration of the oxidant was varied to obtain different ratios of –OH and CNC. The newly introduced –OH groups facilitate the CNC–NRL interaction, owing to probable hydrogen bonding. In the presence of a base, the reduction of manganese (VII) ions to manganese (VI) ions takes place, which resulted in brown solid manganese (IV) oxide.

Reaction I: $MnO_4^- + H_2O + e^- \longrightarrow MnO_4^{2-}$ (at pH > 7) (1)

Reaction II: $MnO_4^{2-} + H_2O + 2e^- \longrightarrow MnO^2 + 4\ OH^-$ (2)

Manganese (VII) has a typical absorption band in the UV region, with the maximum absorbance at 525 nm, which was utilized to confirm the oxidation reaction. When the oxidation reaction takes place, the manganese (VII) available in the suspension gradually turns to manganese (IV) and the typical purple colour diminishes. When an excess of MnO_4^- exists in the suspension, the purple colour perseveres and it reveals the end of the reaction, owing to the lack of availability of double bonds in the polymer. Figures 7 and 8 show the UV–Vis spectra of the NRL suspension after the oxidation reaction and the $KMnO_4$ solution used for the oxidation, respectively. The presence of the peak at 525 nm is noted in the spectrum of the $KMnO_4$ solution, but not in that of the NRL suspension, confirming the complete usage of the reagent.

Measurements of mechanical properties

Tensile property tests were performed on the films formed from NRL, and NRL with 2% CNCs and with 4% CNCs. The results are shown in Table 2. Positive results were achieved, as expected. Tensile strength and tensile modulus were noted to increase with the increase in CNC concentration, while the elongation at break decreases with the increase in CNC content. The –OH groups in NRL chains favour the interaction of the matrix with CNCs, which helps in the transfer of stress, which could be the reason for the observed increase in mechanical properties of the materials.

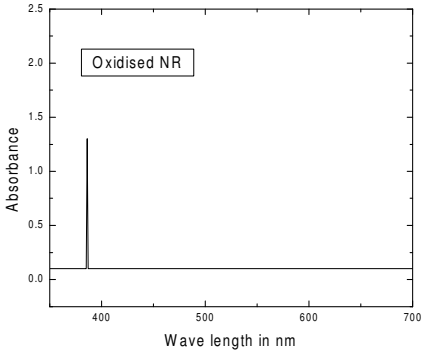

Figure 7: UV-visible spectrum of oxidised NR latex

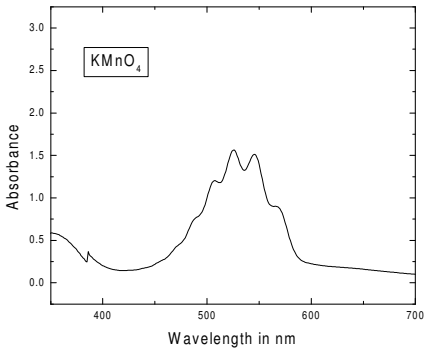

Figure 8: UV-visible spectrum of $KMnO_4$

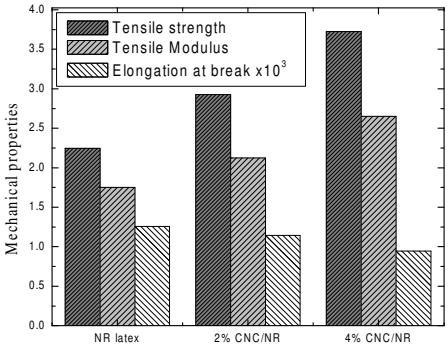

Figure 9: Graphical representation of mechanical properties of NRL, 2% CNC/NR and 4% CNC/NR

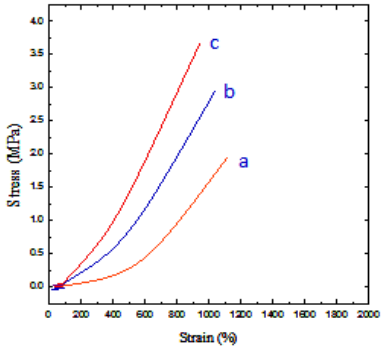

Figure 10: Stress-strain curves of (a) NRL, (b) 2% CNC/NR and (c) 4% CNC/NR

Table 2
Mechanical properties of NRL, 2% CNC in NRL and 4% CNC in NRL

Sample	Tensile strength (M Pa)	Tensile modulus (M Pa)	Elongation at break (%)
NR latex	2.2468	1.7525	1258.56
2% CNC in NR	2.9263	2.1248	1145.23
4% CNC in NR	3.7246	2.6523	946.53

Estimation of dye removal ability

UV-visible spectroscopy was used to analyse the untreated and treated model wastewater. The percentage removal was determined using the formula:

$$A_0 - \frac{A_t}{A_0} \times 100 \quad (3)$$

where A_0 is the absorbance of the dye solution filtered with the latex membrane and A_t is the absorbance of the dye solution filtered with the composite membrane.

The absorbance of each dye was noted at their λ_{max}, using the UV-vis spectrophotometer. The optical absorbance of the dyes Victoria blue BO, Methyl violet 10B and Holacryl pink FG was observed at 583, 529 and 618 nm, respectively, by UV–Vis spectroscopy to determine the percentage removal of the dyes. A stock solution of model wastewater was prepared by adding dyes (10 mg/L) in deionized water to determine the adsorption of the dyes onto the uncross-linked and cross-linked membranes. The composite membranes, cut into pieces of 25 × 15 mm, were incubated for 24 h in the model wastewater solution of pH 5, at room temperature (25 ± 2 °C), under stirring. The latex membrane was chosen as the control for measuring the adsorption of the dyes onto the composite membranes by the method stated above. The experiments were conducted in the absence of light to avoid photo-depletion.

Table 3
Effect of type of dye on the percentage removal of dyes

Type of dye	Percentage removal of dyes
Victoria blue BO	92 ± 2.1
Methyl violet 10B	79 ± 1.9
Holacryl pink FG	67 ± 1.2

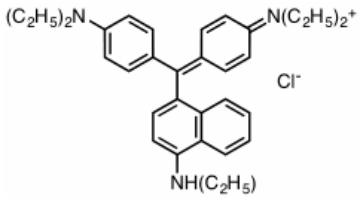

Figure 11: Structure of Victoria blue BO

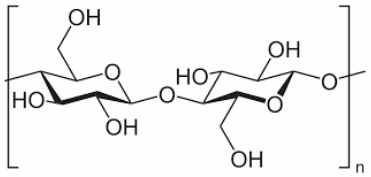

Figure 12: Structure of cellulose

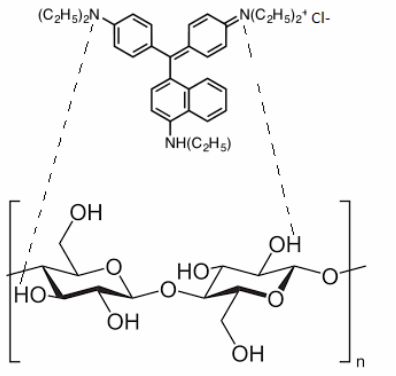

Figure 13: Binding mechanism of the dye to CNCs through hydrogen bonding

CONCLUSION

Cellulose nanocrystals were prepared successfully from bleached wood pulp and were characterised using FTIR and XRD. Natural rubber latex was oxidised using $KMnO_4$. The oxidation facilitated the interaction between CNCs and NRL. Successful casting of CNC embedded NRL composite films, with 2% and 4% CNC concentration, was achieved and supported using FTIR, XRD, SEM and UV-Vis analysis techniques, as well as by assessing the mechanical properties of the materials. The obtained films showed enhanced mechanical properties. It is expected that the developed CNC embedded NRL films can be used as an economic upgrade in the water purification industry. Due to the abundant surface hydroxyl groups of CNCs, which can be exchanged with almost any contaminant ions present in wastewater, such materials can serve as filtration membranes in the water purification industry. Moreover, the enhanced mechanical properties of the novel composite support their proposed application in the water purification industry.

REFERENCES

[1] J. Bandyopadhyay, *Int. J. Water Resour. Dev.*, **4**, 411 (1995).
[2] A. K. Biswas and C. Tortajada, *Int. J. Water Resour. Dev.*, **2**, 129 (2010).
[3] C. P. Leo, M. Z. Yahya, S. N. M. Kamal, A. L. Ahmad and A. W. Mohammad, *Water Sci. Technol.*, **4**, 831 (2013).
[4] D. R. Paul and L. M. Robeson, *Polymer*, **15**, 3187 (2008).
[5] R. Lin, B. V. Hernandez, L. Ge and Z. Zhu, *J. Mater. Chem.*, **2**, 293 (2018).
[6] W. Wang, A. Sedykh, H. Sun, L. Zhao, D. P. Russo *et al.*, *ACS Nano*, **12**, 12641 (2017).
[7] X. Q. Zhang, X. Xu, N. Bertrand, E. Pridgen, A. Swami *et al.*, *Adv. Drug Deliv. Rev.*, **13**, 1363 (2012).
[8] D. Trache, M. H. Hussin, M. K. M. Haafiz and V. K. Thakur, *Nanoscale*, **5**, 1763 (2017).
[9] R. Singla, A. Guliani, A. Kumari and S. Yadav, *Nanocellulose and Nanocomposites*, **5**, 103 (2016).
[10] K. J. De France, T. Hoare and E. D. Cranston, *Chem. Mater.*, **1**, 4609 (2017).
[11] X. Zhuo, C. Liu, R. Pan, X. Dong and Y. Li, *ACS Sustain. Chem. Eng.*, **5**, 4414 (2017).

[12] P. Liu, K. Oksman and A. P. Mathew, *J. Colloid Interface Sci*., **464**, 175 (2016).
[13] H. Sehaqui, A. Mautner, U. P. de Larraya, N. Pfenninger, P. Tingaut *et al*., *Carbohyd. Polym.*, **135**, 334 (2016).
[14] L. Jin, W. Li, Q. Xu and Q. Sun, *Cellulose*, **4**, 2443 (2015).
[15] V. K. Thakur and S. I. Voicu, *Carbohyd. Polym*., **146**, 148 (2016).
[16] H. Voisin, L. Bergström, P. Liu and A. P. Mathew, *Nanomaterials*, **3**, 57 (2017).
[17] C. Zhu, I. Dobryden, J. Rydén, S. Öberg, A. Holmgren *et al*., *Langmuir*, **45**, 12390 (2015).
[18] R. Wang, S. Guan, A. Sato, X. Wang, Z. Wang *et al*., *J. Membrane Sci*., **446**, 376 (2013).
[19] B. Chen, Q. Zheng, J. Zhu, J. Li, Z. Cai *et al*., *RSC Adv*., **99**, 96518 (2016).
[20] Y. Hao, Z. Wang, Z. Wang and Y. He, *Ecotoxicol. Environ. Saf*., **168**, 298 (2019).
[21] X. Zheng, X. Li, J. Li, L. Wang, W. Jin *et al*., *Int. J. Biol. Macromol. A*, **107**, 283 (2018).
[22] G. Biliuta, D. Suteu, T. Malutan, A.-I. Chirculescu, I. Nica *et al*., *Cellulose Chem. Technol*., **52**, 609 (2018).
[23] L. A. de S. Costa, A. F. Fonseca, F. V. Pereira and J. I. Druzian, *Cellulose Chem. Technol*., **2**, 127 (2015).
[24] M. Rahimi Kord Sofla, R. J. Brown, T. Tsuzuki and T. J. Rainey, *Adv. Nat. Sci*: *Nanosci. Nanotechnol*., **3**, 1 (2016).